

Hard X-ray submicrometer tomography of human brain tissue at Diamond Light Source

This content has been downloaded from IOPscience. Please scroll down to see the full text.

2017 J. Phys.: Conf. Ser. 849 012030

(<http://iopscience.iop.org/1742-6596/849/1/012030>)

View [the table of contents for this issue](#), or go to the [journal homepage](#) for more

Download details:

IP Address: 131.152.231.249

This content was downloaded on 04/07/2017 at 11:26

Please note that [terms and conditions apply](#).

You may also be interested in:

[Three-dimensional cellular and subcellular structures of human brain tissue determined by microtomography](#)

Ryuta Mizutani, Akihisa Takeuchi, Susumu Takekoshi et al.

[Effect of vitro preservation on mechanical properties of brain tissue](#)

Wei Zhang, Yi-fan Liu, Li-fu Liu et al.

[Ultrasonic Absorption Anomaly of Brain Tissue](#)

Akinori Etoh, Shigeki Mitaku, Jun Yamamoto et al.

[Potentiometric Dye Imaging for Pheochromocytoma and Cortical Neurons with a Novel Measurement System Using an Integrated Complementary Metal–Oxide–Semiconductor Imaging Device](#)

Takuma Kobayashi, Ayato Tagawa, Toshihiko Noda et al.

[Dynamical properties of the brain tissue under oscillatory shear stresses at large strain range](#)

F Boudjema, B Khelidj and M Lounis

[Imaging electric properties of human brain tissues by B1 mapping: A simulation study](#)

Xiaotong Zhang and Bin He

[3D characterization by tomography of beta Al₉Fe₂Si₂ phase precipitation in a Al_{6.5}Si₁Fe alloy](#)

D Ferdian, L Salvo, J Lacaze et al.

[Development of the system for visualization of electric conductivity distribution in human brain and its activity by the magnetic induction tomography \(MIT\) method](#)

S Sapetsky, V Cherepenin, A Korjnevsky et al.

Hard X-ray submicrometer tomography of human brain tissue at Diamond Light Source

A Khimchenko¹, C Bikis¹, G Schulz¹, M-C Zdora^{2,3}, I Zanette²,
J Vila-Comamala², G Schweighauser⁴, J Hench⁴, S E Hieber¹,
H Deyhle¹, P Thalmann¹ and B Müller¹

¹ Biomaterials Science Center, Department of Biomedical Engineering, University of Basel, Allschwil, CH.

² Diamond Light Source, Harwell Science & Innovation Campus, Didcot, Oxfordshire OX11 0DE, UK.

³ Department of Physics & Astronomy, University College London, London WC1E 6BT, UK.

⁴ Institute of Pathology, Department of Neuropathology, Basel University Hospital, Basel, CH.

E-mail: anna.khimchenko@unibas.ch

Abstract. There is a lack of the necessary methodology for three-dimensional (3D) investigation of soft tissues with cellular resolution without staining or tissue transformation. Synchrotron radiation based hard X-ray in-line phase contrast tomography using single-distance phase reconstruction (SDPR) provides high spatial resolution and density contrast for the visualization of individual cells using a standard specimen preparation and data reconstruction. In this study, we demonstrate the 3D characterization of a formalin-fixed paraffin-embedded (FFPE) human cerebellum specimen by SDPR at the Diamond-Manchester Imaging Branchline I13-2 (Diamond Light Source, UK) at pixel sizes down to 0.45 μm . The approach enables visualization of cerebellar layers (*Stratum moleculare* and *Stratum granulosum*), the 3D characterization of individual cells (Purkinje, stellate and granule cells) and can even resolve some subcellular structures (nucleus and nucleolus of Purkinje cells). The tomographic results are qualitatively compared to hematoxylin and eosin (H&E) stained histological sections. We demonstrate the potential benefits of hard X-ray microtomography for the investigations of biological tissues in comparison to conventional histology.

1. Introduction

The most common cell imaging technique is microscopy of stained tissue sections. It can be a simpler set up like a hematoxylin and eosin (H&E) stained sections for classical optical microscopy, or a more complex one like labelling with fluorescent dyes or antibody staining for epifluorescence or confocal microscopy. Advanced microscopy approaches have been successfully applied to study the three-dimensional (3D) cerebellar microstructure [1, 2]. The main disadvantage of these methods is the requirement for a chemical agent to obtain information on the cellular level, whose use may have effects on the tissue morphology.

X-ray tomography can overcome some disadvantages of the histology, providing high-resolution 3D data of a comparable quality, without staining and non-destructively. Synchrotron radiation based grating interferometry enabled the identification of non-stained Purkinje cells [3, 4]. As it was recently demonstrated, the synchrotron radiation based in-line tomography allows for the 3D characterization down to subcellular structures [5]. Thus, X-ray microtomography



is emerging as a promising solution for the visualization of cellular structures in 3D, offering a simpler specimen preparation, shorter experiment time and complexity, compared to histology, albeit at the cost of inferior lateral spatial resolution.

In-line phase contrast X-ray tomography [6–8] with single distance phase recovery (SDPR) using Paganin's methods [9] is one of the simplest phase contrast methods [10] in terms of data acquisition, as it is based only on free-space propagation of X rays between specimen and detector [11]. In this study, we demonstrate the 3D characterization of a formalin-fixed paraffin-embedded (FFPE) human cerebellum specimen by synchrotron radiation based SDPR at the Diamond-Manchester Imaging Branchline I13-2 (Diamond Light Source, UK) [12] at pixel sizes down to 0.45 μm . The approach enables the visualization of cerebellar layers (*Stratum moleculare* and *Stratum granulosum*), individual cells (Purkinje, stellate and granule cells) and subcellular structures (nucleus and nucleolus of Purkinje cells). The tomographic results are qualitatively compared to H&E-stained histological sections.

2. Materials and methods

2.1. Tissue preparation

The *post mortem* human cerebellum specimen was extracted from a 73-year-old male. The specimen preparation was performed according to the standard histological protocols [5], but without the staining procedure. All procedures were conducted according to the Declaration of Helsinki and approved by the Ethikkommission Nordwestschweiz. After paraffin embedding the tomography specimen 4.0 mm in height and 2.6 mm in diameter was extracted from a histological cassette by a metal punch.

2.2. Synchrotron radiation based in-line single distance tomography

Tomography experiments were performed at the Diamond-Manchester Imaging Branchline I13-2. Two scans of the same specimen were acquired. A monochromatic X-ray beam with a photon energy of 19 keV was extracted from a silicon $\langle 111 \rangle$ double crystal monochromator. After being transmitted through the sample, the X-ray beam was collected by a scintillator-based X-ray detector pco.4000 (PCO AG, Kelheim, Germany) located at distances of 5 cm and 8.5 cm. The effective pixel size was set by the optical magnification of the detector to 0.45 μm for the propagation distance of 5 cm and to 1.1 μm for the propagation distance of 8.5 cm. Propagation distances were selected based on the contour plot for used pixel sizes and photon energy [13]. The measurement with 0.45 μm pixel size was performed in a local tomography configuration as the sample diameter was bigger than the detector field of view for the selected magnification. Due to the detector size (4008 \times 2672 pixels), 2400 equiangular projections [14] over 180 degrees with exposure times of 8.00 s and 1.58 s, respectively, were acquired. The exposure time for 0.45 μm measurement was increased in order to preserve comparable photon counts between scans. Data preprocessing and phase recovery were performed using the software tool ANKAphase [13] with an input parameter $\delta/\beta = 2406$ [5] for 1.1 μm effective pixel size and $\delta/\beta = 414$ for 0.45 μm effective pixel size. The second δ/β was decreased in comparison to theoretical value for paraffin in order to reduce gradient artefact in the data. The tomographic reconstruction was done in Matlab R2014b (Simulink, The MathWorks, Inc., USA).

2.3. Histology

A comparable cerebellum specimen was investigated by means of histology. A section of 4 μm thickness was cut using a microtome, mounted on a glass slide, and stained with H&E. Image of the resulting slide was taken on a light microscope with optical magnification 60 \times . The histological section was cropped around the region of interest and registered to the selected region of the tomography slice with the effective pixel size of 1.1 μm using the Demon registration tool [15] with affine transformation constraint (rotation and scaling).

2.4. Data registration

The tomographic datasets were registered using an automatic 3D/3D registration tool [16, 17] with rigid transformation constraints. The SDPR with effective pixel size $0.45\ \mu\text{m}$ was set as the reference dataset.

3. Results and discussion

Figure 1 shows selected slices of non-registered and registered FFPE human cerebellum measured with effective pixel sizes of $1.1\ \mu\text{m}$ (A, B) and $0.45\ \mu\text{m}$ (C). Magnifications (E, F) visualize subcellular structures, such as nuclei of Purkinje cell. The microstructure of the human brain is comparably recognized in histology and tomography. Analysing the magnified images in Figure 1 (D-E) one can conclude that already with an effective pixel size of $1.1\ \mu\text{m}$ tomography is comparable to histological sectioning in terms of cellular structure visualization. The image with a pixel size of $0.45\ \mu\text{m}$ demonstrates the potential to surpass H&E-stained histology in terms of subcellular structures.

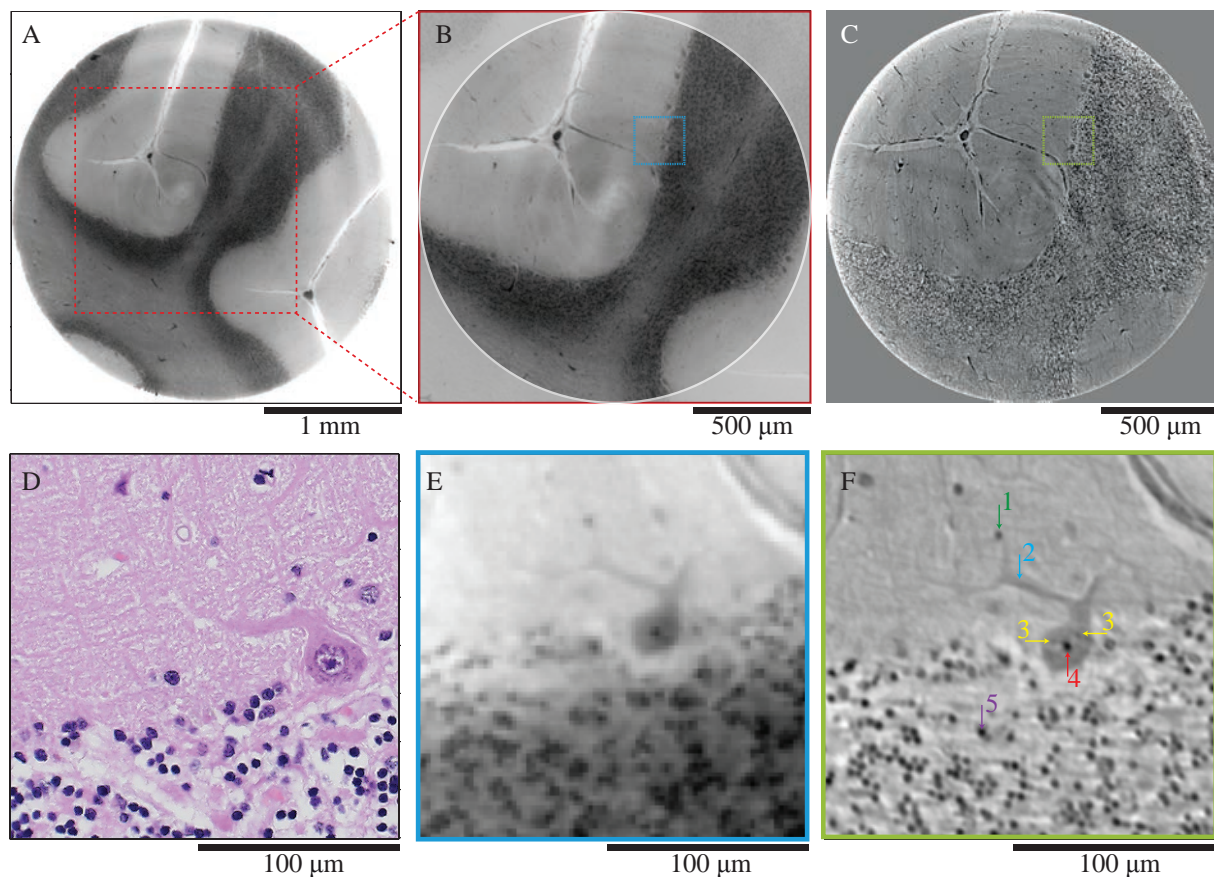


Figure 1. FFPE human cerebellum slices with magnifications highlighting an individual Purkinje cell. Selected tomography slices measured with effective pixel sizes of $1.1\ \mu\text{m}$ (non-registered: A and registered: B) and $0.45\ \mu\text{m}$ (C) with magnifications (E, F) and cropped histological section (D). Green (1): stellate cell; Blue (2): dendrite of Purkinje cell; Yellow (3): dense structure within nucleus of Purkinje cell; Red (4): nucleolus of Purkinje cell; Violet (5): granular cell.

Figure 1 (D-F) show a large Purkinje cell with an average diameter of $30\ \mu\text{m}$ situated between

the *Stratum granulosum* and *Stratum moleculare*. The Purkinje cell axon takes off after axon hillock and branches further in the *Stratum moleculare*.

While the spatial resolution of the data with the effective pixel size of 0.45 μm is superior with respect to the data with the effective pixel size of 1.1 μm , the density contrast is superior in the data with the effective pixel size of 1.1 μm . The decrease of the density contrast of the higher resolution data can be a result of the use of local tomography, in which the regions of the sample outside of the field of view generate a background that may decrease the quality of the reconstruction. The strategy to increase the contrast can lay in data reconstruction with a higher δ/β , although it may cause a radial gradient and image blurring.

Tomography scanning time only accounts for a fraction of the time required for serial sectioning histology. In addition, to produce histological slices, see Figure 1 (D), the sample was sectioned into 4 μm thick sections, stained with H&E and visualized by light microscopy. Preparation steps induce local deformations within the inhomogeneous tissue, which can be corrected during post-processing [18]. To produce 3D data from individual sections a complex volume reconstruction is required [19].

4. Conclusion

We conclude that SDPR can reach the subcellular level, providing a compromise between spatial resolution, density contrast, and penetration depth. We present an approach for the visualization of cells within tissue of relatively large volumes without staining. For the specific case of the cerebellum, the clear visualization of various cell types, including Purkinje cells, stellate cells in *Stratum moleculare* and granule cells in *Stratum granulosum* was demonstrated. While histology still yields superior two-dimensional (2D) image quality, synchrotron radiation based tomography provides a valuable 3D complement.

Acknowledgments

The authors gratefully acknowledge the financial support of the Swiss National Science Foundation (SNSF) project 147172. The authors highly appreciate the support of the team of Diamond Light Source, Didcot, UK, particularly C Rau and P Thibault.

References

- [1] Benard M *et al* 2015 *J. Vis. Exp.* **99** 52810
- [2] Wang H *et al* 2014 *NeuroImage* **84** 1007-17
- [3] Schulz G *et al* 2010 *J. R. Soc. Interface* **7** 1665-76
- [4] Schulz G *et al* 2012 *Sci. Rep.* **2** 826
- [5] Hieber S E *et al* 2016 *Sci. Rep.* **6** 32156
- [6] Snigirev A *et al* 1995 *Rev. Sci. Instrum.* **66** 548692
- [7] Cloetens P *et al* 1996 *J. Phys. D: Appl. Phys.* **29** 13346
- [8] Zanette I *et al* 2013 *Appl. Phys. Lett.* **103** 244105
- [9] Paganin D *et al* 2002 *NeuroImage* **206** 3340
- [10] Lang S *et al* 2014 *J. Appl. Phys.* **116** 154903
- [11] Krenkel M *et al* 2016 *AIP Advances* **6** 035007
- [12] Rau C *et al* 2011 *Phys. Stat. Sol.* **A208** 2522-25
- [13] Weitkamp T *et al* 2011 *J. Synchrotron Rad.* **18** 617-29
- [14] Holme M, *et al* 2014 *Nat. Protoc.* **9** 140115
- [15] Dirk D-J *et al* 2009 *Proc. ISBI* **1** 963-6
- [16] Andronache A *et al* 2008 *Med. Image Anal.* **12** 315
- [17] Müller B *et al* 2012 *Int. J. Mater. Res.* **103** 242-249
- [18] Germann M *et al* 2008 *J. Neurosci. Methods* **170** 14955
- [19] Krauth A *et al* 2010 *NeuroImage* **49** 2053-62